Journal of Ceramic Processing Research. Vol. 21, No. 4, pp. 508~514 (2020)
(Received 18 March 2020, Received in revised form 27 March 2020, Accepted 2 April 2020)
https://doi.org/10.36410/jcpr.2020.21.4.508

J O U R N A L O F
Ceramic Processing Research

Hydrogen production from methane steam reforming over Mg modified nickel-based catalyst: Process optimization

Shian Li[a], Zhiyu Yao[b], Facai Yang[a], Guogang Yang[a,*] and Qiuwan Shen[a]
[a]*Marine Engineering College, Dalian Maritime University, Dalian, China*
[b]*Harbin Guanghan Gas Turbine Co. Ltd., Harbin, China*

Methane steam reforming (MSR) reaction is a promising industrial hydrogen production technology. Mg-Ni/CeO_2 catalysts at different Mg/Ni ratios of 6/4, 7/3, 8/2 and 9/1 with total loading of 10 wt% were used as catalysts for hydrogen production. The characterization techniques such as XRD, SEM and EDS were carried out on fresh and spent samples. Results showed that the optimum Mg addition content for Mg/Ni-CeO_2 is 2%. The process optimization of reaction parameters were conducted by evaluating the catalytic activity. The stability of optimal Mg-Ni/CeO_2 catalyst at 700 °C is examined for 8 h on-stream reaction. It reveals that Mg/Ni-CeO_2 still maintains a relatively high catalytic activity after 8 h stability test.

Keywords: hydrogen production, Methane steam reforming, Mg addition, Ni-CeO_2.

Introduction

An increase in the global policies related to the generation of green energy has stimulated the use of alternative energy sources and the development of several technologies that will help to replace the dependency on fossil fuels [1, 2]. Compared with new energy sources such as solar energy and wind energy, hydrogen is a secondary energy source that can be produced in a wide variety of ways, such as photolysis of water, electrolysis of water, chemical looping hydrogen production and hydrocarbon reforming [3]. The most mature hydrogen production technology is the hydrocarbon reforming which has the characteristics of low cost and high hydrogen production rate.

Methane reforming is a widely used technique in industries to convert natural gas to hydrogen or syngas [4]. According to different reforming raw materials, it can be divided into partial oxidation of methane [5], carbon dioxide reforming of methane [6-7] and steam reforming of methane [8-9]. Methane steam reforming (MSR) reaction is an endothermic reaction and is a fairly mature industrial hydrogen production technology.

Noble metal catalysts such as Rh, Ru, Pd and Pt with high activity, stability and carbon deposition resistance have been investigated intensity [10-12]. Among many traditional metal catalysts, Ni-based catalysts stand out due to their lower cost, good catalytic and higher stability performance at high temperatures [13-15]. The support is one of the essential components of the catalyst. The nature of the support is crucial in the catalytic performance of supported metal catalysts. For some specific reactions, besides affecting metal dispersion and providing stability to the metal particles, the support can also participate in the reactions [16-17]. The support is required to have high mechanical strength, large specific surface area and strong anti-sintering ability. In general, ceria has been widely used in heterogeneous catalysis due to its unique properties [18].

Several types of materials have been studied for MSR. And it was reported that intermediate metal loading can significantly improve the catalytic performance [19-21]. Nickel-based catalysts with different metallic contents supported on ceria-zirconia were studied by Dong et al. [19]. They found that the optimal amount of nickel loading is 15%.Roh et al. studied the effect of nickel content on a Ce-ZrO_2/Al_2O_3 support. The result showed that when the nickel content is 12% wt., the conversion rate of methane is the maximum [20].

In this work, we have studied different Ni contents and Mg addition to optimize their composition as catalysts in MSR. A series of catalysts were synthesized by wet incipient wetness impregnation method and thoroughly characterized by XRD, SEM and EDS. The effects of the Ni loading and Mg addition on reactivity of the catalysts were investigated to achieve a deeper understanding on Mg-Ni/CeO_2 catalysts. In addition, the optimal reaction conditions were studied by evaluating the effect of reactivity temperature, the gas hourly space velocity (GHSV) and H_2O/CH_4 (S/C) molar ratios.

*Corresponding author:
Tel : +86-13050561150
Fax: +0411-84728659
E-mail: yanggg@dlmu.edu.cn

Materials and Methods

Samples preparation

Preparation of different wt% Ni loadings catalysts

Wet incipient wetness impregnation method was used to prepare the catalysts. First, $Ni(NO_3)_2 \cdot 6H_2O$ having a corresponding Ni loading amount was weighed into a beaker, and CeO_2 was used as a support. Deionized water was added to $Ni(NO_3)_2 \cdot 6H_2O$ according to the measured water absorption rate of the support to prepare a precursor solution. When the $Ni(NO_3)_2 \cdot 6H_2O$ was completely dissolved, the precursor solution and the CeO_2 support were immersed, mixed vigorously with a stirrer for 15 minutes to achieve homogenous absorption of Ni solution over the surface of CeO_2. Standing at room temperature for 12 hours, then the composite was aged at 110 °C for 12 h inside, taken out and ground, and finally calcined at 500 °C for 5 hours in a muffle furnace. The Ni loadings were 6.0 wt%, 8.0 wt%, 10.0 wt% and 12.0 wt% respectively.

Preparation of Mg-Ni/CeO_2

$Mg(NO_3)_2 \cdot 6H_2O$ having a corresponding Mg doping amount was weighed into a beaker and dissolved in a certain amount of deionized water. Then immerse the solution in the prepared Ni/CeO_2. Standing at room temperature for 12 hours, then the composite was aged at 110 °C for 12 h inside. The composite was aged at 110 °C for 12 h inside, taken out and ground, and finally calcined at 500 °C for 5 hours in a muffle furnace. The Mg doping were 1.0 wt%, 2.0 wt%, 3.0 wt% and 4.0 wt% respectively.

Evaluation of catalytic activity

The catalytic activity of the catalysts was carried out in a fixed bed system at atmospheric pressure. The catalyst was pretreated for 2~3 hours at 500 °C under hydrogen stream. The reducing mixture gas was composite of H_2 and Ar (H_2: Ar=1:9, 300 mL/min) and brought in at a ramp rate of 10 °C/min from room temperature to 500 °C. The schematic diagram of the fixed bed quartz reactor is shown in Figure 1. The system is divided into three parts: a feeding unit, a methane steam reforming reactor and an analysis part.

Characterization

Powder X-ray diffraction data (XRD) were collected in the Philips X'Pert PRO of PANalytical B.V. with Cu Kα radiation (λ = 0.1542 nm) and a 2θ range of 10-90° to study the crystalline structure of the samples. The morphologies of the synthesized catalysts were studied by scanning electron microscopy (SEM, SUPRA 55 SAPPHIRE).

Experimental result evaluation and analysis method

The following definitions were used for evaluation of the catalyst performance:

Conversion of methane was calculated as follows:

$$CH_4\ (\%) = \frac{CH_4\ (\text{inlet}) - CH_4\ (\text{outlet})}{CH_4\ (\text{inlet})} * 100\%$$

Hydrogen generation rate expression:

$$H_2\ (\%) = \frac{H_2\ (\text{outlet})}{CH_4\ (\text{inlet}) - CH_4\ (\text{outlet})} * 100\%$$

Carbon monoxide selective expression:

$$CO_{selectivity}\ (\%) = \frac{CO\ (\text{outlet})}{CO\ (\text{inlet}) + CO_2\ (\text{outlet})} * 100\%$$

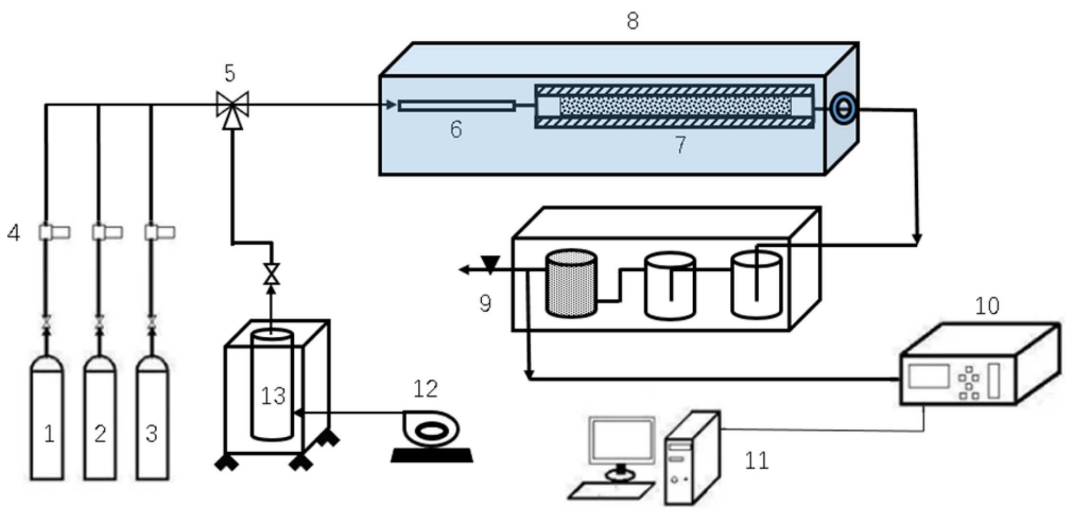

Fig. 1. Schematic diagram of the fixed bed quartz reactor system (1. Methane 2. Nitrogen 3. Hydrogen 4. Mass flow meter 5. Three-way valve 6. Preheating pipe 7. Reactor 8. Tube furnace 9. Exhaust gas treatment device 10. Online infrared gas composition and calorimeter 11. Computer Control 12. Water Pump 13. Steam Generator).

Results and Discussion

Characterizations

XRD diffraction results of Ni/CeO_2 with different Ni loading of 6-12 wt% are shown in Figure 2. It can be seen that there are characteristic peaks of NiO at 2θ = 43.5°, 50.8°, and 75°, and characteristic peaks of CeO_2 exist at 2θ = 33.1°, 38.5°, 56.6°, 67.7° and 83.7°. Figure 3(a)-3(c) displayed the SEM image, elemental mapping and EDS analysis of 10% Ni/CeO_2. It validates the existence of Ni on the surface of CeO_2. The EDS spectrum and chemical composition of Ni/CeO_2 are given in Table 1. It demonstrates that the fraction of Ni in Ni/CeO_2 is smaller than CeO_2.

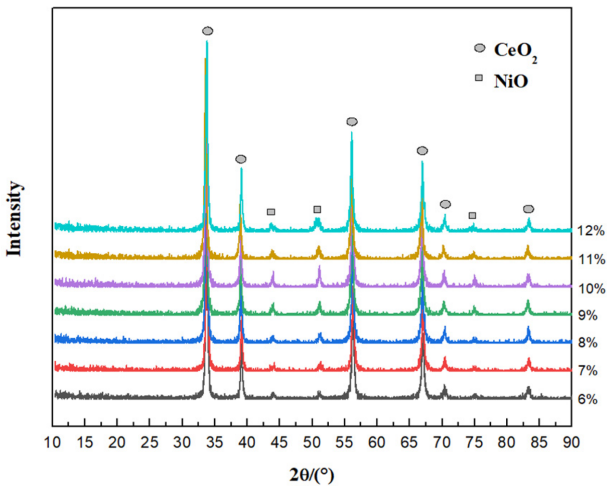

Fig. 2. XRD patterns of catalysts with different Ni loadings.

Catalytic performance

Effect of loading amount on catalytic activity of Ni/CeO_2

This part mainly investigates the effect of different Ni loadings on the catalytic activity of Ni/CeO_2 with Ni content varying from 6% to 12% (Temperature = 700 ºC; n(H_2O): n(CH_4) = 3; and GHSV = 1000 h^{-1}).

Figure 4 shows the comparison of catalytic capability with different Ni loadings. It can be concluded that the conversion rate of CH_4 increase with the increase of Ni loading from 6% to 10%, the hydrogen yield also increase obviously. When the value of the Ni loading reaches 10%, the hydrogen yield reaches the highest value of 182.1%, and the CH_4 conversion rate reaches to 73.6%. However, CH_4 conversion rate and the hydrogen yield all decrease when the Ni loading continued increasing until 12%. For the CO selectivity,

Table 1. EDS analysis results of 10% Ni/CeO_2

Element	O K	Ni K	Ce L
Wt (%)	18.81	17.54	63.65
Atomic (%)	60.96	15.49	23.55

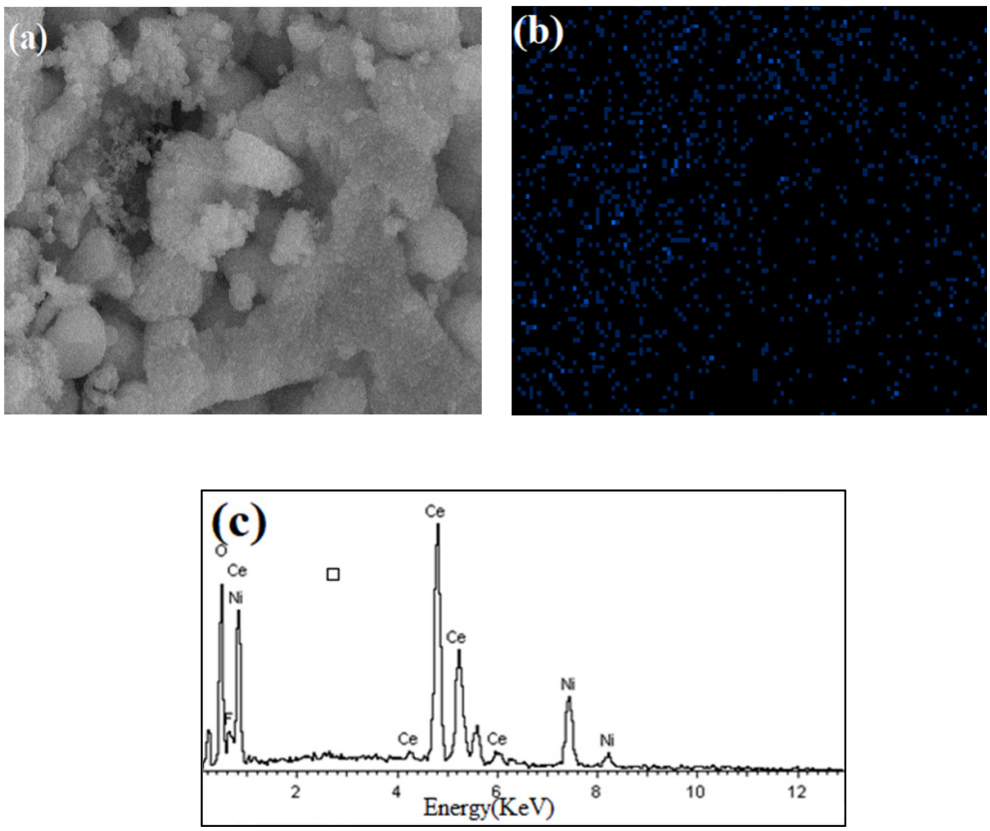

Fig. 3. (a) SEM image of Ni in 10% Ni/CeO_2; (b) Elemental mapping; (c) EDS analysis of 10% Ni/CeO_2.

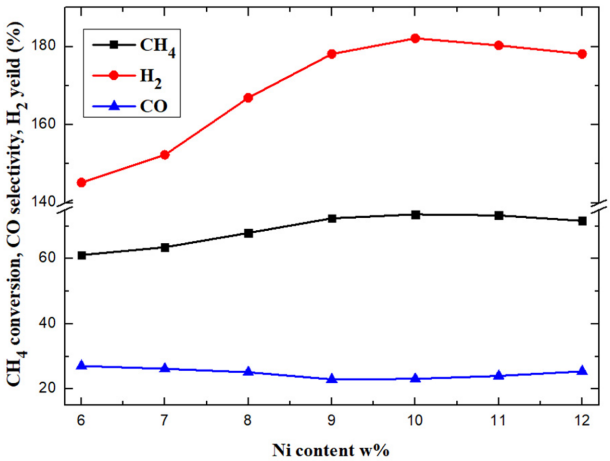

Fig. 4. Catalytic properties of catalysts with different Ni loadings.

it decreases first and then increases with the increase of Ni loading. The minimum value of CO selectivity is 22.97% for the catalyst with 9% Ni loading. The above results demonstrate that the Ni content and dispersion have significant effect on the catalytic properties. There is an optimum nickel content in the nickel based catalyst, which allows all the active components to disperse uniformly on the active site of the support surface without aggregation [20].

Effect of Mg and Sr addition

In this part, comparison of catalytic performance of Mg/Ni-CeO_2 and Sr/Ni-CeO_2 with different Mg/Sr additions are studied (Temperature = 700 °C; $n(H_2O)$: $n(CH_4)$ = 3; and GHSV = 1000 h^{-1}).

It can be seen from Figure 5 that the addition of Mg contributes the methane conversion rate of Ni-CeO_2 from 73.6% to 74.9%. However, the addition of Mg deceases the CO selectivity from 23.1% to 20.4%. The hydrogen yield has the optimal value when 2% of Mg was added. The addition of Mg inhibits the formation of CO_2, thereby reducing the water vapor reaction, meanwhile the methane conversion rate increases significantly. Thus the value of hydrogen production also shows an increasing trend. Overall, the addition of Mg has a definite influence for the activity of the catalyst. According to the above analysis, it is conclude that the optimum value of Mg addition for Ni/CeO_2 catalysts is 2%.

It can be seen from Figure 5 that the nickel-based catalyst with the addition of 2% Sr has a methane conversion rate from 73.6% to 75.2%. However, with the increase of the Sr addition amount, the H_2 yield shows a downward trend and the CO selectivity shows an upward trend, indicating that the addition of Sr increases the poisoning of the catalyst, which is not conducive to long-term work of the catalyst.

Morphology characterization of Mg/Ni-CeO_2

Figure 6a shows that the surface morphology of Mg/

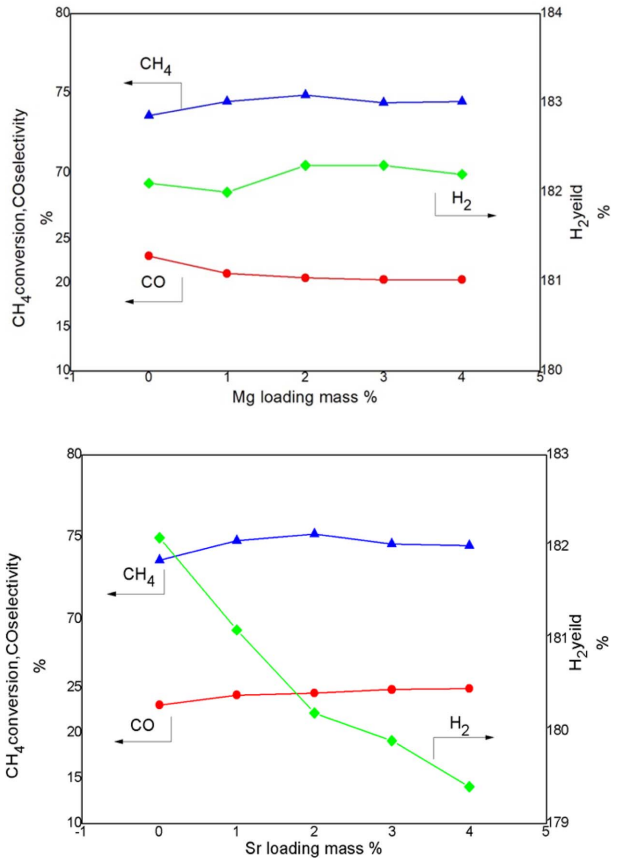

Fig. 5. Comparison of catalytic performance Ni-CeO_2 with different Mg/Sr additions.

Ni-CeO_2 is porous. The dispersion is high and there is no agglomeration or sintering. From Figure 6b, it can be seen that the crystal of NiO can still be observed on the surface of the Mg/Ni-CeO_2 after the reaction. No carbon filaments are observed in the SEM. It can be inferred that the carbon diffusion rate at the surface metal-carbon interface of the catalyst is at a low level, so that Mg/Ni-CeO_2 is considered to have high carbon deposition resistance and stability [20].

Effect of Temperature

The effect of temperature on the activity performance of catalysts are investigated at the following conditions: Mg-Ni/CeO_2 with a Ni loading of 10%, Mg addition of 2%, 1 atm, $n(H_2O)/n(CH_4)$ = 3, and GHSV = 1000 h^{-1}.

As shown in Figure 7, it is clear that the CH_4 conversion rate, H_2 yield and CO selectivity all increase with the increasing temperature. CH_4 conversion rate increases from 31.6% to 75.2%, and reaches the maximum value at 750 °C. The methane conversion rate changes slightly at the temperature above 700 °C. The hydrogen yield increases from 139.7% to 182.3%, reaching the maximum value at 700 °C. CO selectivity increases from 8.5% to 21.2%, reaching the maximum value of 21.2% at 750 °C. Considering the life of pipelines and the energy consumption, 700 °C is the

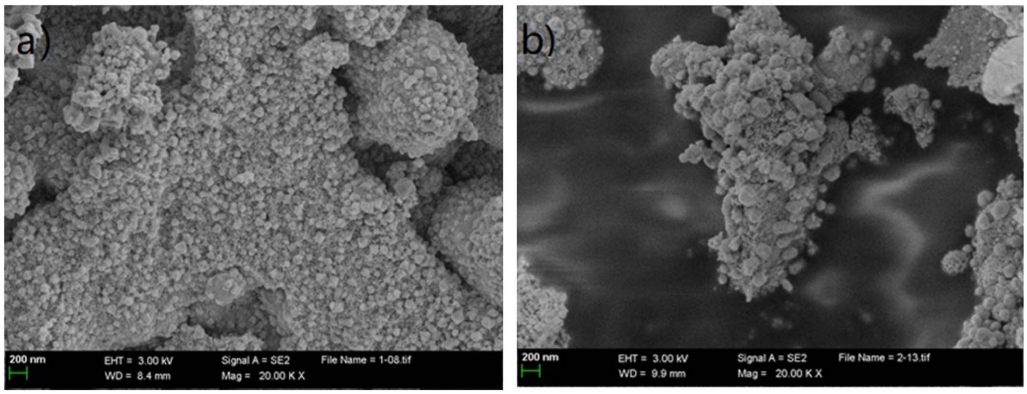

Fig. 6. SEM image of the Mg/ Ni-CeO_2 catalysts (a) fresh sample (20000×); (b) spent sample (20000×).

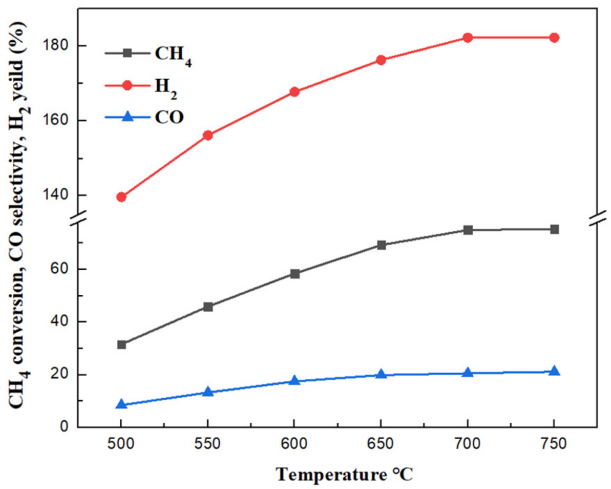

Fig. 7. Effect of temperature on the activity performance of catalysts.

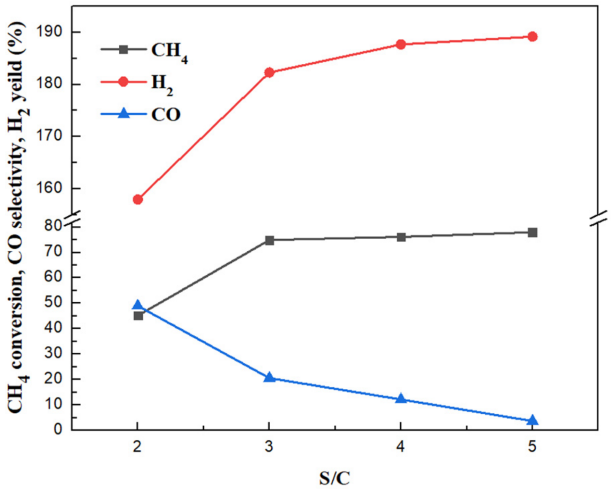

Fig. 8. Effect of S/C on the activity performance of catalysts.

optimum reaction temperature in the study. Under this reaction condition, the CH_4 conversion rate is 74.9%, the H_2 production rate is 182.3%, the CO selectivity is 20.6%.

Effect of S/C

The effect of H_2O/CH_4 ratios (S/C) on the activity performance of catalysts are investigated at the following conditions: Mg-Ni/CeO_2 with a Ni loading of 10%, Mg addition of 2%, 700 ºC, 1 atm, and GHSV = 1000 h^{-1}.

It can be seen from Figure 8 that an increase of the S/C ratio results in an increase of methane conversion rate, hydrogen yield, and a decrease of carbon monoxide selectivity. When the S/C ratios increase from 2 to 3, the CH_4 conversion rate increases from 45.2% to 74.9%, the hydrogen yield increases from 157.9% to 182.3%, and the CO selectivity ranges from 49% to 20.6%; When the S/C ratios increase from 3 to 5, the CH_4 conversion rate and hydrogen yield continue to increasing but they change slightly, while CO decreased to 3.66%.

Increasing the amount of water vapor in the reaction leading the active oxygen atom which on the surface of the nickel-based catalyst reacting with the active quaternary carbon atom and carbon monoxide to form CO_2. The cleavage of reactive functional groups such as methine and methylene groups accelerating the methane cracking. Previous studies have confirmed the enhancement of water vapor partial pressure on the MSR reaction, indicating that the water vapor promoted the rapid decline of CO selectivity [17]. However, excessive water vapor consumption requires a large amount of energy. From the economic point of view, the S/C ratio is not as high as possible. In this study, the S/C ratio of 3 is considered as the optimum value.

Effect of GHSV

In this part, Mg-Ni/CeO_2 with a Ni loading of 10%, Mg addition of 2% was studied under the reaction conditions: 700 ºC; S/C = 3; 1 atm. The gas hourly space velocity (GHSV) of methane is used as the standard, and the methane input is =100 SCCM. The GHSV of each experiment is controlled by changing the catalyst loading. The calculation formula is:

$$GHSV = V_{CH_4}/V_{Ni/CeO_2}$$

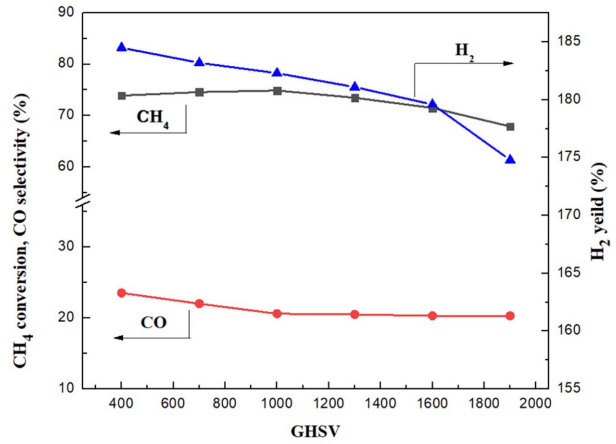

Fig. 9. Effect of GHSV on the activity performance of catalysts.

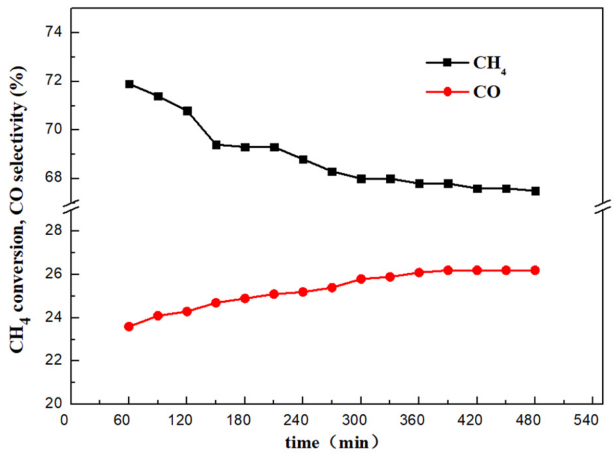

Fig. 10. Stability of Mg-Ni/CeO_2 catalysts for SRM, Reaction conditions: T = 700 °C (8 h), GHSV = 1000 h^{-1}, S/C = 3.

It can be seen from Figure 9 that in the lower GHSV region (400 h^{-1}~1000 h^{-1}), the CO selectivity decreases from 23.51% to 20.6% with the increase of GHSV, and the methane conversion rate fluctuates between 73.9% and 74.9%. The hydrogen yield dropped from 184.5% to 182.3%. The selectivity of CO remained unchanged when the GHSV continued to increase. However when the GHSV increases to 1900 h^{-1}, the methane conversion rate decreases to 67.9%, and the hydrogen yield has the same trend. In this study, the GHSV of 1000 h^{-1} is considered as the optimum value.

Stability tests

Catalyst with a Ni loading of 10% and a Mg addition content of 2% was used for the stability test. Experiment was conducted to evaluate the stability of the catalyst at 700 °C for 8 hours under flow ($n(H_2O)$: $n(CH_4)$ = 3, and GHSV = 1000 h^{-1}). Results are shown in Figure 10. During this period, the catalysts show good stability at 700 °C where the beginning of highest CH_4 conversion is observed. It can be concluded that Mg/Ni-CeO_2 still maintains a relatively high catalytic activity after 8 h stability test.

Conclusions

Mg-Ni/CeO_2 catalysts at different Mg/Ni ratios of 6/4, 7/3, 8/2 and 9/1 with total loading of 10 wt% were synthesized via a wetness impregnation method and applied for MSR. The characterization techniques such as XRD, SEM and EDS were carried out on fresh and spent samples. Results showed that the optimum Mg addition content for Mg/Ni-CeO_2 is 2%. The process optimization of reaction parameters were conducted by evaluating the catalytic activity. Finally, the stability test for 8h at 700 °C demonstrated the excellent thermal stability of the resulted Mg/Ni-CeO_2 catalysts.

Acknowledgments

This work was supported by the National Natural Science Foundation of China Funding (No.51779025 and No.51606013), China Postdoctoral Science Foundation Funding (No.2019M651097 and No. 2019M 651094), Fundamental Research Funds for the Central Universities of China (No.3132019187, No.3132019191 and No.3132019327), and Natural Science Foundation of Liaoning Province (No.2019-BS-026 and No.2019-ZD-0154).

References

1. S.A. Li, J.L. Yuan, G.N. Xie, and B. Sunden, Int. J. Hydrog. Energy 43 (2018) 8451-8463.
2. Q.W. Shen, S.A. Li, G.G. Yang, J.L. Yuan, N.B. Huang, J. Ceram. Process. Res. 20 (2019) 152-157.
3. J.H. Hwang, and K.T. Lee, J. Ceram. Process. Res. 21[1] (2019) 57-63.
4. T.L. LeValley, A.R. Richard, and M. Fan, Int. J. Hydrog. Energy 39 (2014) 16983-17000.
5. A.C.W. Koh, L. Chen, W.K. Leong. B.F.G. Johnson, T. Khimyak, and J. Lin, Int. J. Hydrog. Energy 32 (2007) 725-730.
6. M. Rezaei, S.M. Alavi, S. Sahebdelfar, P. Bai, X. Liu, and Z.F. Yan, Appl Catal, B. 77(2008)346-354.
7. M.S. Fan, A.Z. Abdullah, and S. Bhatia, Int. J. Hydrog. Energy 36 (2011) 4875-4886.
8. S. Ali, M.J. Almarri, A.G. Abdelmoneim, A. Kumar, and M.M. Khader, Int. J. Hydrog. Energy 41[48] (2016) 22876-22885.
9. V.K. Jaiswar, S. Katheria, G. Deo, and D. Kunzru, Int. J. Hydrog. Energy 27 (2017) 18968-18976.
10. A. Berman, R.K. Karn, and M. Epstein, Appl. Catal. Gen. 282[1-2] (2005) 73-83.
11. R. Craciun, W. Daniell, H. Kno zinger, Appl. Catal. Gen. 230 (2002) 53-68.
12. V.P. De Souza, D. Costa, D. Dos Santos, A.G. Sato, and J.M.C. Bueno, Int. J. Hydrog. Energy 37[13] (2012) 9985-9993.
13. N. Salhi, C. Petit, A.C. Roger, A. Kienemann, S. Libs, and M.M. Bettahar, Catal. Today 113[3-4] (2006) 187-193.
14. X. Fang, X. Zhang, Y. Guo, M. Chen, W. Liu, and X. Xu,

Int. J. Hydrog. Energy 41 (2016) 11141-11153.
15. R. Martınez, E. Romero, C. Guimon, R. Bilbao, Appl. Catal. Gen. 274[1-2] (2004) 139-149.
16. M. Cargnello, P. Fornasiero, and R.J. Gorte, Catal. Lett. 142 (2012) 1043-1048.
17. M. Ahmadi, H. Mistry, and B.R. Cuenya, J. Phys. Chem. Lett. 7 (2016) 3519 -3533.
18. T. Montini, M. Melchionna, M. Monai, P. Fornasiero, Chem. Rev.116 (2016) 5987-6041.
19. W.S. Dong, H.S. Roh, K.W. Jun, S.E. Park, and Y.S. Oh, Appl. Catal. A Gen. 226 (2002) 63-72.
20. H.S. Roh, K.W. Jun, S.E. Park, Appl. Catal. A Gen. 251 (2003) 275-283.
21. Y.Y. Ji, W.Z. Li, and Y.X. Chen, Natural Gas Chemistry 9[4] (2000) 291-303.